Finite-Element Navier-Stokes Analysis of the Flow About a Finite Plate

Jean Caille* and Joseph A. Schetz†
Virginia Polytechnic Institute and State University, Blacksburg, Virginia

The problem considered is the "classical" case of laminar flow about a finite flat plate over the range $10^2 \leq Re_L \leq 10^5$, treating the whole flowfield with particular emphasis on the leading and trailing edges and the near wake. It was worthwhile to revisit this problem using modern numerical methods for the Navier-Stokes equations because it was found that the agreement between the existing predictions and newer experiments is surprisingly poor for some key features of the flow. The present work uses a weak Galerkin formulation for the finite-element method with the pressure determined by a penalty approach. The results are presented mainly in terms of the skin-friction coefficient on the plate, the wake centerline velocity variation, and the velocity variation along the upstream stagnation streamline. Thick plates are also considered. The results are compared to earlier analyses and experiments. Finally, the case of a three-dimensional finite width ($L = W$) flat plate at $Re_L = 10^2$ and 10^3 is treated and discussed.

Nomenclature

C_f	= skin-friction coefficient
DX	= width of the element
DY	= height of the element
FP	= surface of the plate
L	= plate length
LE	= leading edge
n_j	= normal vector
P	= pressure
R_i	= residuals
Re_L, Re	= Reynolds number based on L
t_i	= surface traction
T	= plate thickness
TE	= trailing edge
u,v,w	= velocity components
U_i, U, V, W	= u/L, v/L, w/L
x,y,z	= axial, vertical, and transverse coordinates
X,Y,Z	= x/L, y/L, z/L
λ	= penalty parameter
ρ	= fluid density
μ	= fluid viscosity

Subscripts

Cl	= values along axis of symmetry
top	= external boundary above the plate
up	= upstream region
∞	= freestream conditions

Introduction

THE analysis of laminar flow about an aligned flat plate goes back to the early years of the century when Prandtl[1] developed the boundary-layer theory for high Reynolds number flows and Blasius[2] solved the semi-infinite flat-plate problem. Since that time, some experiments and a number of analytical and numerical studies have been done to better understand the characteristics of the flow in various regions, e.g., the upstream, plate, and wake regions. (See Refs. 3–34.) By studying this list, one can notice certain important facts. First, very few experiments exist. It is hard to perform a good and complete experiment, especially at low Reynolds numbers, due to the physical limitations of wind tunnels, models, and instruments. Second, this fundamental problem is clearly not so simple. One has to be very careful about the treatment of the leading- and trailing-edge regions. There are also a number of parameters to be considered—Re_L, plate thickness, etc. Third, the agreement between the existing theoretical and numerical predictions and the experiments is surprisingly poor for some key features of the flow.[23] Finally, one finds very few three-dimensional (e.g., finite width) studies in the literature.[30–32] For these reasons, it was decided to revisit this general flow problem using modern numerical methods for the full Navier-Stokes equations.

The specific purpose of this paper is to study the laminar, incompressible flow about an aligned finite plate for Reynolds numbers based on the length of the plate (Re_L) between 10^2 and 10^5, treating the whole flowfield with particular emphasis on the leading and trailing edges and the near wake, for the three geometrical cases of thin, thick, and finite-width plates. The numerical method is the finite-element method (FEM). A weak Galerkin formulation with the pressure determined by a penalty approach was used. This method was chosen for three reasons: 1) this method has been successfully applied many times to the Navier-Stokes equations for other kind of problems—it is efficient and robust; 2) the boundary conditions can be applied very efficiently for this type of flow—it is easy with the FEM to combine essential and natural boundary conditions; and 3) the FEM is convenient for different geometries.

Equations of Motion

The mathematical model for the laminar flow of an incompressible fluid is given by the continuity equation and the Navier-Stokes equations as

$$U_{i,i} = 0$$

$$\rho U_j U_{i,j} = -P_{,i} + \mu[U_{i,j} + U_{j,i}]_{,j}$$

Finite-Element Method

The present work uses a weak Galerkin formulation for the FEM with the pressure determined by a penalty approach. The

Presented as Paper 87-1442 at the AIAA 19th Fluid Dynamics, Plasma Dynamics, and Lasers Conference, Honolulu, HI, June 8–10, 1987; received June 22, 1987; revision received Feb. 29, 1988.

*Graduate Assistant, Aerospace and Ocean Engineering Department. Student Member AIAA.

†W. Martin Johnson Professor and Department Head, Aerospace and Ocean Engineering Department. Fellow AIAA.

complete details of this formulation are readily available in other references (e.g., Ref. 35); thus, only an outline of the technique is presented here.

Substitution of an approximate solution (U^*,P^*) into the equations yields a set of residual equations of the form

Momentum:

$$f_1(U^*,P^*) = R_1$$

Continuity:

$$f_2(U^*) = R_2$$

where R_i are the residuals, a measure of the quality of the approximate solution. The Galerkin method reduces this error to zero, in a weighted sense, by making the residuals orthogonal to some set of functions. The weighting functions δU_i must satisfy the continuity equation. The continuity equation constraint is enforced by use of a penalty method. The resulting weak formulation is given by

$$\int_D [\delta U_i \rho U_j U_{i,j} + \delta U_{i,j}\mu(U_{i,j} + U_{j,i}) + \lambda U_{i,i}\delta U_{i,i}]\, dD = \int_S \delta U_i t_i\, dS$$

where λ is a positive number whose value affects the accuracy of the solution. A value of λ of 10^6-10^8 usually proves effective. When the divergence theorem is applied, it introduces the natural boundary conditions involving the surface tractions t_i:

$$t_i = [-P + \mu(U_{i,j} + U_{j,i})]n_j$$

The pressure appears only implicitly through the surface integrals on the right-hand side. The only unknowns are the velocity components. Once the velocity field is obtained, the pressure may be computed in a postprocessing step from the relationship

$$P = -\lambda U_{i,i}$$

The formulation results in a system of nonlinear algebraic equations of the form

$$[K(U)](U) = (F)$$

where K is the global system matrix, U the global vector of unknown velocities, and F the global vector of known boundary conditions. The following strategy was found suitable to solve this system of equations. Starting from a first guess for the velocity field, the successive substitution method is used to reduce the error inside the radius of convergence of the Newton-Raphson method that is used to iterate until final convergence. The linearized system of equations is solved by direct Gaussian decomposition in a compacted, skyline, out-of-core solver.

For two-dimensional flows, the biquadratic velocity, bilinear pressure element was used and, for three-dimensional flows, the trilinear velocity, constant-pressure element was chosen for reasons of computational economy.

Results and Discussion

One of the most important factors in doing a numerical analysis of an external flow problem is the design of the computational region and the grid. The domain should be as small as possible to keep a reasonable mesh size, but it must be large enough to provide a realistic description of the flow. The criteria used in this work have been chosen after many tests.

One of the advantages of the FEM is the implementation of the boundary conditions. One can use both essential (e.g., specify/values for the velocities) and natural (e.g., specify values for the surface tractions) boundary conditions. Our earlier experience for unbounded flows, such as a free laminar jet that is very sensitive to outer boundary conditions, has demonstrated the great utility of "traction-free," i.e., $t_i = 0$ outer boundary conditions. This allows for unrestrained inflow or outflow through the outer boundaries and is thus much less constraining on the flow than other boundary conditions such as $u = U_\infty$, $v = 0$, and $p = P_\infty$. Also, with this type of external condition and a Navier-Stokes treatment, no "interaction" analysis is necessary.

For low Reynolds numbers ($Re_L \leq 1200$), it was found that an acceptable solution could be computed with a relatively coarse mesh: 41 points in the streamwise direction and 15 points in the normal direction. For the higher Re_L (≥ 3000), a finer mesh was required due to the high gradients in the viscous region. For the three-dimensional flows, a coarse mesh ($41 \times 15 \times 15$) was used due to the limitations in the storage and the CPU time. For all the meshes, it was crucial to use clustering of the nodes near the plate in the normal direction and near the leading and trailing edges for the streamwise direction.

All the computations were executed on an IBM 3090 with vector facility. The maximum total CPU time for the computation of a two-dimensional flow was 70 s. It was with a 91×31 node mesh for four iterations: two successive substitutions and two Newton-Raphson. For the three-dimensional flows with a $41 \times 15 \times 15$ node mesh, the total CPU time was about 90 min using the same strategy. For the three-dimensional flows, it was necessary to access a virtual machine of 12 megabytes of memory and to use 320 megabytes of disk storage. The FEM computer code used was the convenient and well-tested FIDAP.[36]

Two-Dimensional Flat Plate

The first problem treated is the two-dimensional flow about a thin plate of finite length. Figure 1 shows the computational region and the boundary conditions. The location of the upstream and top boundaries are dependent on the Reynolds number. For the upstream boundary, the following criterion was used:

$$-Re_{X_{up}} > 200$$

where this Reynolds number is based on the distance from the leading edge. This choice is based in part on the results of Walter and Larsen.[27] In their study, the decay of the upstream

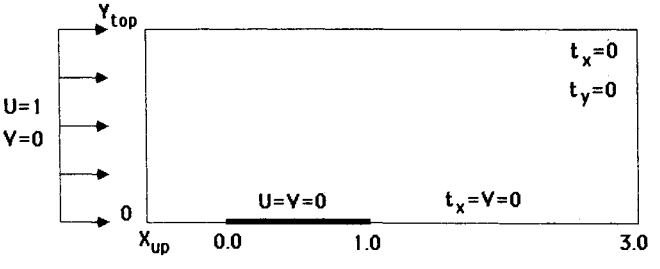

Fig. 1 Computational region and boundary conditions for the two-dimensional finite flat plate.

Table 1 Characteristics of the domain and mesh for the two-dimensional finite flat plate

Re	X_{up}	Y_{top}	$DX(LE)$	$DX(TE)$	$DY(FP)$	Grid
100	−2.00	1.000	0.000200	0.000200	0.000198	77 × 21
400	−1.00	0.500	0.000170	0.000200	0.000162	77 × 21
1,000	−0.50	0.400	0.000130	0.000200	0.000124	77 × 21
1,200	−0.50	0.400	0.000130	0.000200	0.000124	77 × 21
3,000	−0.20	0.250	0.000080	0.000200	0.000076	77 × 21
10,000	−0.10	0.110	0.000008	0.000200	0.000066	91 × 31
100,000	−0.10	0.110	0.000008	0.000200	0.000066	91 × 31

velocity was found to begin at a value of about 100. In some computational tests, some variations in the results were significant with that criteria. Therefore, it was decided to increase the value to 200. For larger values of X_{up} than the one based on the above criterion, no major differences were observed for the upstream centerline velocity distribution.

The top boundary is located at about two times the boundary-layer thickness predicted by the Blasius solution. For this case also, some tests were run with larger values of Y_{top} as much as twice the chosen value and no major differences were observed for all the features of the flow including the pressure. The pressure distributions were virtually identical and the peak values agreed to within a few percent. For the wake boundary, a constant location two plate lengths after the trailing edge was used. The location of this boundary is primarily dependent on how far one wants to see results in the wake. For the top and wake boundaries, traction-free conditions were employed.

It was found that a well-behaved solution could be obtained with a 41 × 15 node mesh for the lower Reynolds number, but it was decided to use a finer grid to maximize the accuracy of

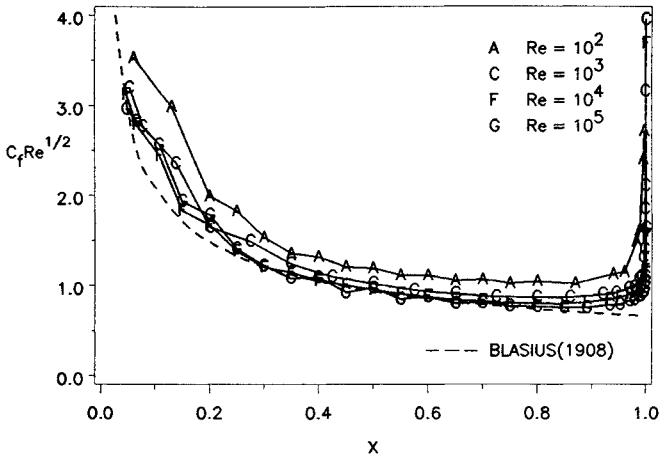

Fig. 2 Skin-friction coefficient on the two-dimensional finite flat plate.

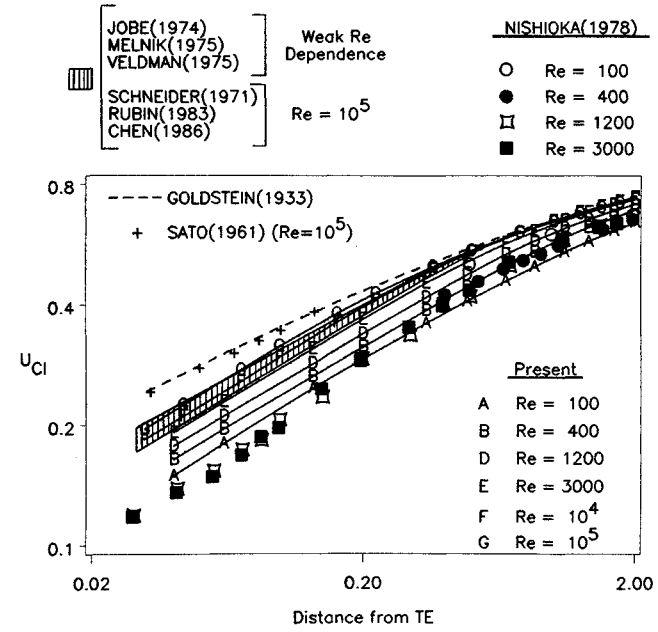

Fig. 3 Wake centerline velocity of the two-dimensional finite flat plate.

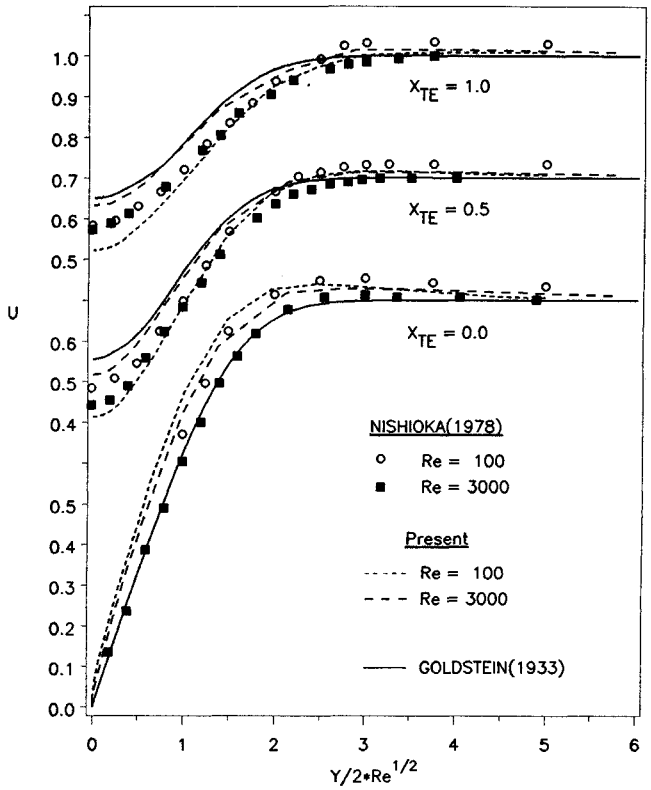

Fig. 4 Wake velocity profiles of the two-dimensional finite flat plate.

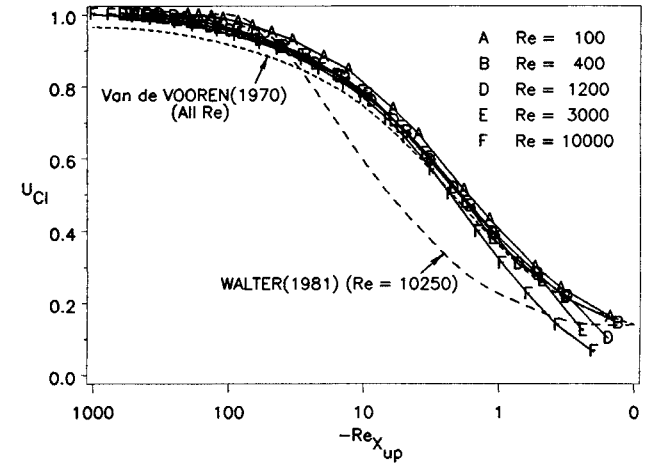

Fig. 5 Velocity variation on the stagnation streamline ahead of the two-dimensional finite flat plate.

Table 2 Comparison of skin-friction coefficient ratio for the two-dimensional finite flat plate at $X = 0.8$

	C_f/C_f (Blasius[2])	
Re	Present	Asymptotic[a]
100	1.409	1.240
400	1.225	1.200
1,000	1.170	1.170
1,200	1.166	1.160
3,000	1.141	1.140
10,000	1.081	1.090
100,000	1.033	1.040

[a]Jobe and Burggraf.[19]

the solution for the skin-friction coefficient and for the near wake. A 77 × 21 mesh was used for Re_L smaller than 3000 and a 91 × 31 mesh for $Re_L = 10^4$ and 10^5. The grids are nonuniform with clustering near the plate and the leading and trailing edges. A geometric increase in nodal spacing was used. The values of the first element size are shown in Table 1.

The current results for Re_L = 100, 400, 1000, 1200, 3000, 10^4, and 10^5 are shown in Figs. 2-5 and in Table 2. The normalized skin-friction coefficient along the plate is given in Fig. 2. For the lower Reynolds numbers, C_f is much higher than the boundary-layer prediction. As Re_L is increased, the agreement is progressively closer, as might be expected. Also, the anticipated rise near the trailing edge due to the wake-induced pressure is obtained. Table 2 shows the results for the ratio of the computed C_f and the value of C_f predicted by Blasius at station $X = 0.8$. Those results are compared with the ones extracted from the asymptotic analysis of Jobe and Burggraf.[19] The agreement is very good for high Re_L but becomes poor for lower Re_L. Globally, the results are in good agreement with the asymptotic and other numerical results for high Reynolds numbers. The range of applicability in terms of Reynolds number of the asymptotic theories is much smaller than has been claimed.

The value of C_f is computed using a second-order accurate approximation for the derivative of the streamwise velocity. Because of the very small spacing near the plate, a small error can be amplified when doing numerical differentiation. This is the main reason for the oscillations, especially near the leading edge where high velocity gradients exist. The flowfield solutions themselves are smooth. For the total drag coefficient of the plate as a function of the Reynolds number, very good agreement with the asymptotic theory and with the experiments of Janour[5] was achieved.

Next, the results for the near wake are given in Figs. 3 and 4. This region of the flow has been the subject of considerable prior study. In Fig. 3, the present predictions for the variation of the centerline velocity in the wake are presented along with the available experimental data and the predictions of other analyses. The comparisons justify the earlier assertion that the predictions of previous analyses are in poor agreement with the recent experiments of Nishioka and Miyagi.[23] The present numerical results are in good agreement with the experiments at lower Re_L. As Re_L increases, our results agree more with the asymptotic and interacting boundary-layer theories. It is possible that our disagreement with the experiments at high Re_L range is due to difficulties with the experiments. They had to use a thicker plate at the same time as the boundary layer at the trailing edge was becoming thinner. The equations and numerical techniques used here are applicable over the whole Reynolds number range. Some comparisons of the velocity profiles at different stations in the wake are presented in Fig. 4. These results support the conclusions reached above. Also, note the correct prediction of the overshoot in velocity.

The flow upstream of the leading edge has attracted much less study in the past. The present results are plotted along with two earlier analyses on Fig. 5. One can see a better overall agreement with the asymptotic theory proposed by Van de Vooren and Dijkstra,[17] except far from the leading edge where the current results approach the numerical results of Walter and Larsen.[27] The theory of Van de Vooren was aimed primarily at the merging of the leading-edge solution smoothly into the downstream boundary-layer flow (see introduction in Ref. 17). The claims for the accuracy of the methods used are all cast in terms of the flowfield in that region of the flow, not the upstream flow far ahead of the plate. It is perhaps important to note that their results for the flow far upstream seem to be asymptotic to a value less than the correct value of 1.0 or, at least, the approach to the upstream flow is much slower than indicated by physical intuition. The results of Walter and Larsen[27] appear strange in the near field ahead of the plate, where they seem to asymptote to a value higher than the correct value of 0.0 as $X \to 0$.

Two-Dimensional Plate with Thickness

The difference noted above between the current results for the infinitely thin plate and the experiments for the higher Re_L can be attributed in part to the thickness and geometry of the

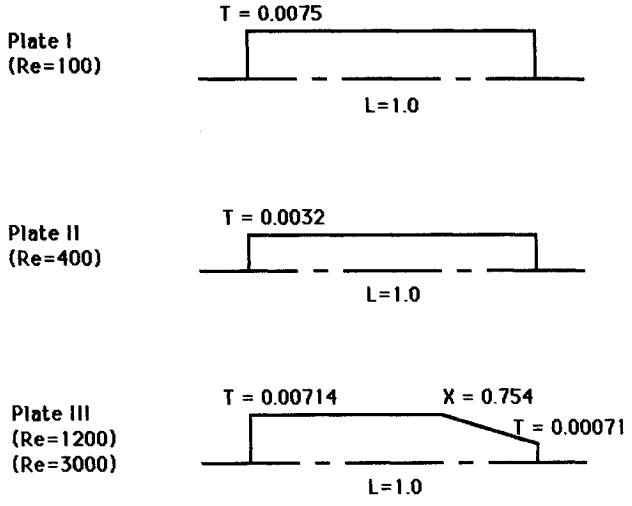

Fig. 6 Thick plate geometries used to model the plates in the experiments of Ref. 23.

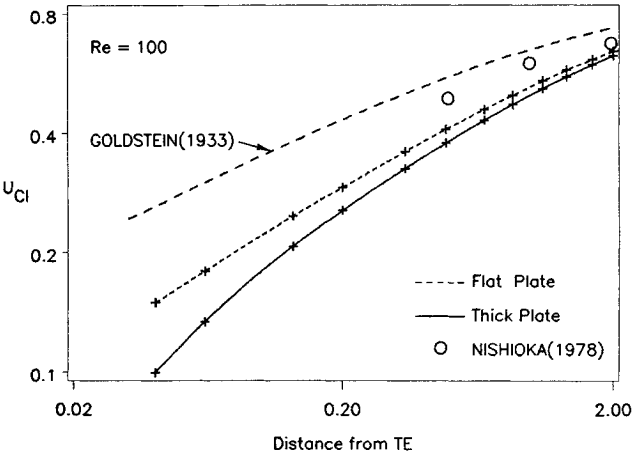

Fig. 7 Wake centerline velocity of two-dimensional finite flat and thick plates at Re = 100.

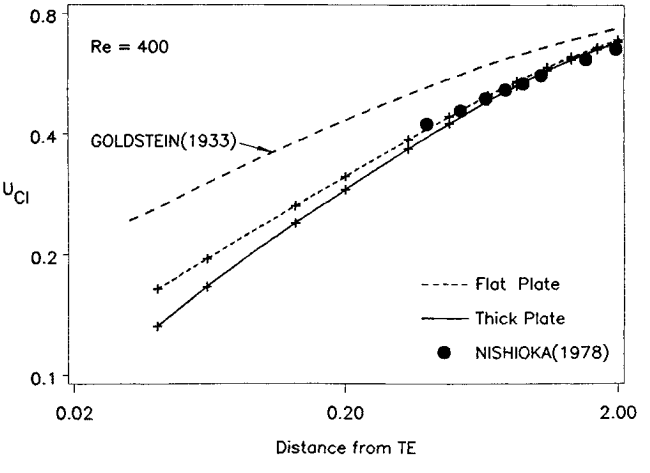

Fig. 8 Wake centerline velocity of two-dimensional finite flat and thick plates at Re = 400.

real plates. An effort was thus made to duplicate the experiments numerically.

Figure 6 shows the three computer models used to simulate the experiments at the four Reynolds numbers. The dimensions of the computational domain are the same as for the previous problems, but the number of nodes was increased. For the region above the plate, 21 points are again used; but for the upstream and the wake regions, the number of points in the normal direction was increased to 27 to permit resolution of the flow ahead of and behind the thick plate.

The results for the wake are shown in Figs. 7–10. The influence of the plate thickness is to slow down the recovery of the centerline velocity in the near part of the wake.The thick plate increases the width of the wake region. Hence, the incoming fluid from the outer wake needs more time to reach the centerline. After a certain distance past the plate, the flow overcomes this effect and, in the far wake, the recovery follows the same pattern as for a thin plate. The distance needed to reach the same recovery rate is smaller for higher Re_L. The agreement between computer model predictions and experiments is not perfect, but one can notice a clear improvement achieved by taking into account the thickness of the plate.

It is also possible to make some comparisons with the asymptotic results of Werle and Verdon.[29] In their study of thickness effects for rounded blunt trailing-edge subsonic flows at high Reynolds number, they found the same trends as observed here.

In Figs. 11 and 12, the influence of plate thickness on the skin-friction coefficient and on the upstream velocity are shown. Except near the leading edge, thickness does not have a major effect on C_f. For the upstream flow, the decay of the centerline velocity toward the forward stagnation point is much faster.

Some velocity vector fields in the near wake behind the plate at low Reynolds number are shown in Fig. 13. Note that no actual reverse flow is observed. The highly viscous fluid simply creeps over the corner. No comparisons with experiment could be made. Indeed, such an experiment is now, and probably always will be, impossible to perform. Using the apparatus of Ref. 23 as a reference, one would have to make velocity profile measurements over the near wake behind a plate whose half-thickness is 0.015 mm! In such a case, the computer "experiment" has a strong advantage. The "probe" in a numerical solution does not have inherent physical size limitations.

Three-Dimensional Flat Plate

The final part of the present study concerns the three-dimensional flow past a thin plate of finite length and finite width. The particular case of a square plate was selected.

The computational region and the boundary conditions are shown in Fig. 14. The "construction" of the three-dimensional domain was done by taking the two-dimensional domain for the desired Reynolds number and by extending this

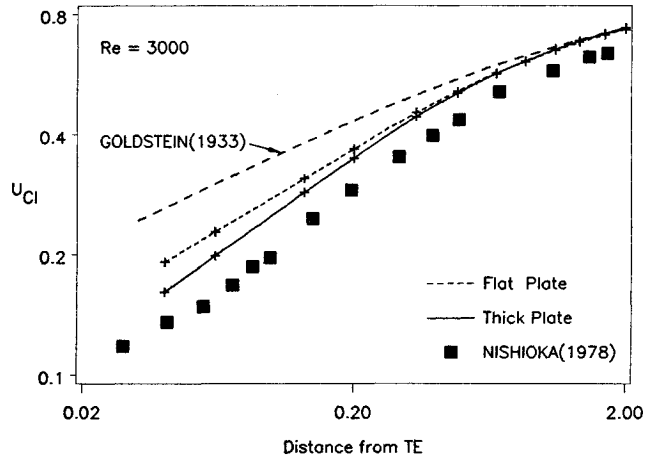

Fig. 10 Wake centerline velocity of two-dimensional finite flat and thick plates at Re = 3000.

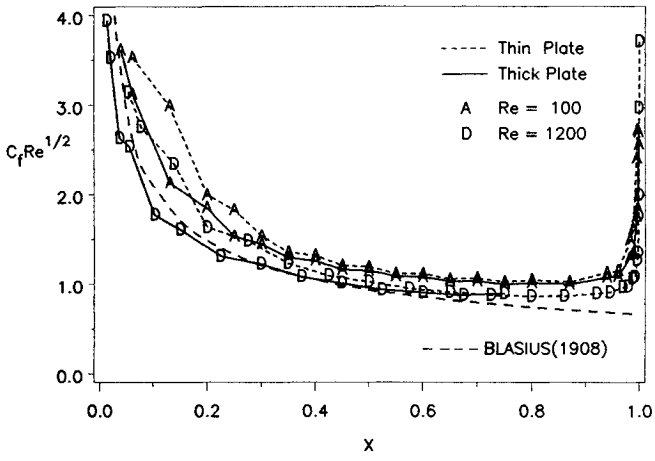

Fig. 11 Skin-friction coefficient of two-dimensional finite flat and thick plates.

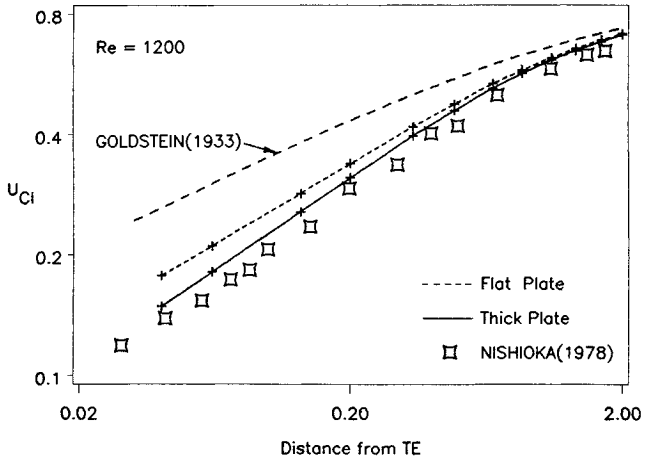

Fig. 9 Wake centerline velocity of two-dimensional finite flat and thick plates at Re = 1200.

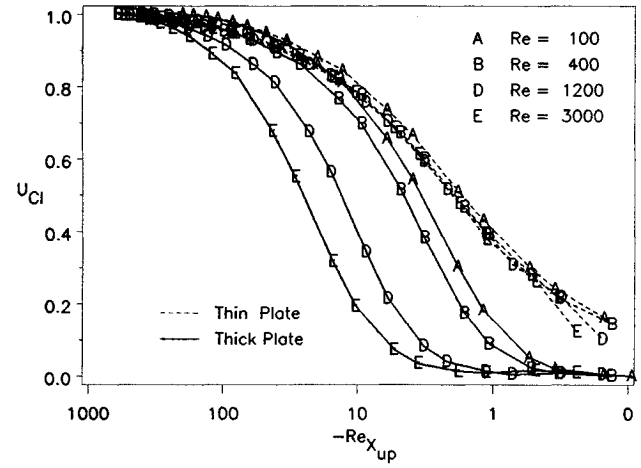

Fig. 12 Velocity variation on the stagnation streamline ahead of two-dimensional finite flat and thick plates.

plane in the Z direction. The side edge of the plate is located at $Z = 0.5$ and the external side edge of the domain is located at $Z = 1.5$ for $Re_L = 10^2$ and at $Z = 1.0$ for $Re_L = 10^3$. A mesh with $41 \times 15 \times 15$ nodes was used for computational economy. This is a relatively coarse mesh, but the adequacy of the three-dimensional results on this mesh was judged by rerunning two-dimensional cases on the same mesh and noting the discrepancies in comparison with two-dimensional results on much finer meshes. The boundary conditions are now applied over planes. For the top, side, and wake planes, traction-free conditions were invoked. For the upstream plane, uniform flow ($U = 1$ and $V = W = 0$) was applied. For the two planes of symmetry, the usual boundary conditions were used —no flow across the plane and traction-free conditions for the other components.

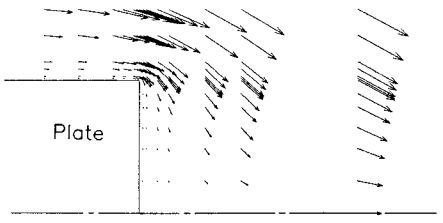

Fig. 13 Velocity vector field near the trailing edge of the two-dimensional finite thick plate at $Re = 100$.

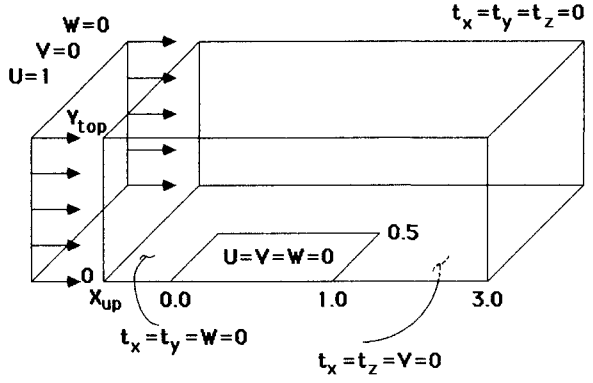

Fig. 14 Computational region and boundary conditions for the three-dimensional finite flat plate.

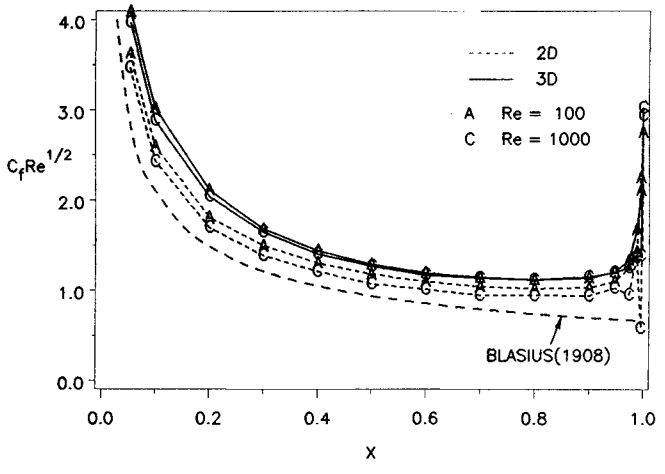

Fig. 15 Streamwise skin-friction coefficient on finite two- and three-dimensional (square) flat plates.

Some results are shown in Figs. 15–19. First, one can compare the results for the midplane with those for the two-dimensional solutions using a 41×15 node mesh with linear elements. The values for C_f over the plate are larger for the three-dimensional flows. This seems reasonable because a part

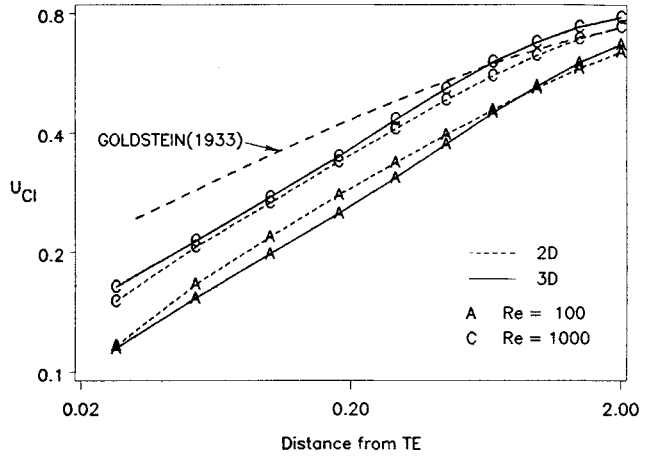

Fig. 16 Wake centerline velocity of finite two- and three-dimensional (square) flat plates.

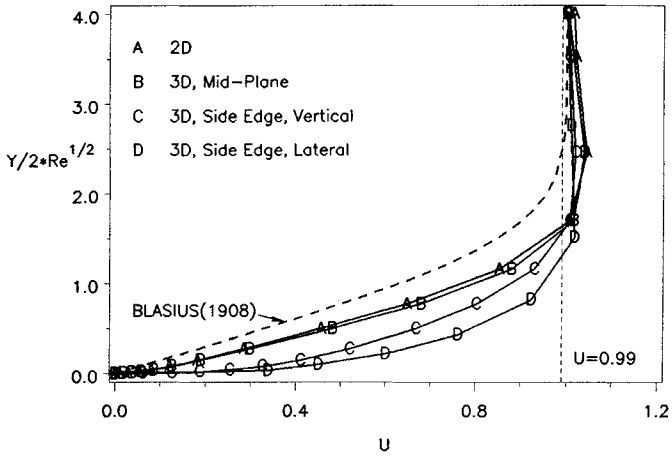

Fig. 17 Velocity profiles at the trailing edge of finite two- and three-dimensional (square) flat plates at $Re = 100$.

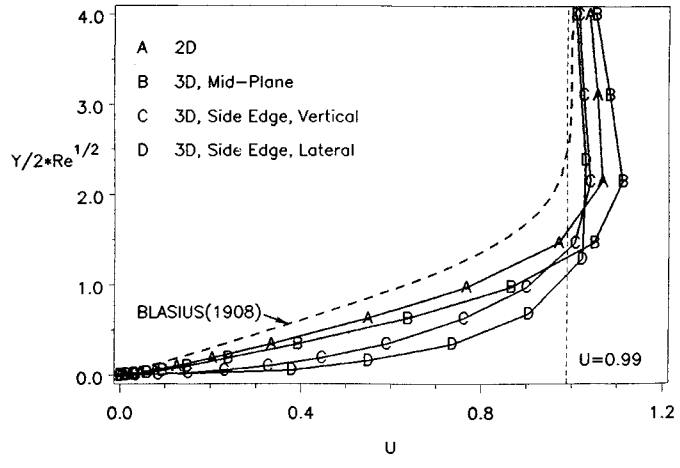

Fig. 18 Velocity profiles at the trailing edge of finite two- and three-dimensional (square) flat plates at $Re = 1000$.

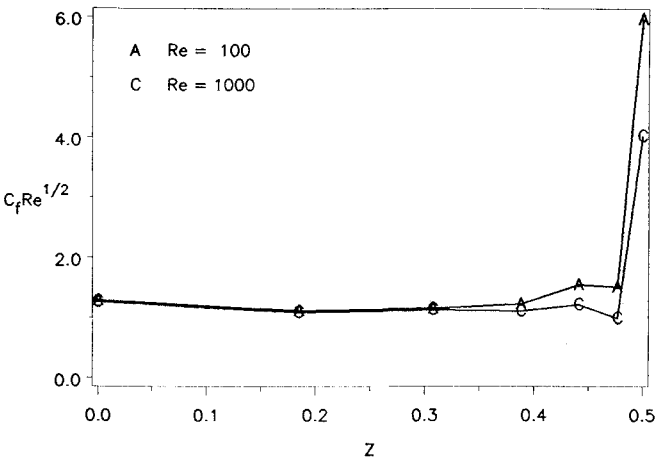

Fig. 19 Streamwise skin-friction coefficient across a three-dimensional finite flat plate at $X = 0.5$.

of the fluid slips away from the plate toward the sides, giving a smaller boundary-layer thickness and therefore higher gradients in the boundary layer. This behavior is in qualitative agreement with the solution of Stewartson and Howarth[31] based on the Oseen approximation. The erratic behavior observable for the two-dimensional results at the higher Re_L is a result of the crude mesh.

The wake centerline velocity is shown in Fig. 16. The three-dimensional results behave roughly similar to the two-dimensional results for the square plate treated. Some differences might be expected, since there will be a lateral flow into the wake from the undisturbed flow to the sides of the plate in the three-dimensional case. Asymptotically, the three-dimensional wake can be expected to evolve into an axisymmetric wake with a different recovery rate than for the planar, two-dimensional wake case.

The next comparison is for the velocity profiles at the trailing edge (Figs. 17 and 18). The profile at the midplane of the plate is compared with the lateral and the vertical profiles on the side edge. Both profiles are much fuller compared to the Blasius[2] (two-dimensional, high Re_L) solution. Also, the boundary-layer thickness on the side is smaller than the one at the midplane. In a paper of Elder,[32] the results of a three-dimensional experiment for $Re_L = 1.06 \times 10^5$ are presented. One of the results found is that the lateral boundary-layer on the side edge is about 0.35 times the vertical boundary-layer at the midplane. For our low Re_L cases, the corresponding ratio is about 0.80. The last comparison is for the streamwise skin-friction coefficient across the plate at the station $X = 0.5$. An increase in C_f as the side edge is reached is shown in Fig. 19 for both Reynolds numbers.

Conclusions

The results obtained indicate that the finite-element method applied to the full Navier-Stokes equations provides a powerful tool for studying the complete flowfield produced by a slender body over a wide range of conditions, $10^2 \leq Re_L \leq 10^5$. The method is efficient and robust, so good solutions with fine meshes can be obtained at reasonable cost for two-dimensional cases. For three-dimensional cases, computer storage and cost considerations still place restrictions on the grid density that can be practically employed, even for large vector machines.

The current comprehensive, two-dimensional numerical results were compared to prior analyses and experiments for parts of the total flow, when available. The comparisons demonstrate that all of the earlier treatments are restricted to only parts of the flow and relatively narrow Reynolds number ranges.

For the three-dimensional case, the literature was found to be very sparse. Our three-dimensional results showed general agreement with the few other approximate analyses or experiments for parts of the flow that could be found. Several interesting features of the flow were found that merit further study.

Acknowledgment

This work was supported mainly by the Office of Naval Research with Dr. H. J. Hansen as Technical Monitor. Support for international cooperation with researchers at the Technical University of Vienna, Austria, was provided by the National Science Foundation.

References

[1]Prandtl, L., "Uber Flussigkeitsbewegung bei sehr kleiner Reibung," *Proceedings of the Third International Congress for Mathematics,* 1904, pp. 484–491 (English translation, NACA TM-452, 1928).

[2]Blasius, H., "Grenzschichten in Flussigkeiten mit kleiner Reibung," *Zeitschift fuer Angewandte Mathematik und Physik,* Vol. 56, No. 1, 1908, pp. 1–37 (English translation, NACA TM-1256, 1950).

[3]Goldstein, S., "Concerning Some Solutions of the Boundary Layer Equations in Hydrodynamics," *Proceedings of the Cambridge Philosophical Society,* Vol. 26, 1930, pp. 1–30.

[4]Goldstein, S., "On the Two-Dimensional Steady Flow of a Viscous Fluid Behind a Solid Body—1," *Proceedings of the Royal Society of London,* Vol. A142, 1933, pp. 545–562.

[5]Janour, Z., "Resistance of a Plate in Parallel Flow at Low Reynolds Numbers," NACA TM-1316, 1951.

[6]Kuo, Y. H., "On the Flow of an Incompressible Viscous Fluid Past a Flat Plate at Moderate Reynolds Numbers," *Journal of Mathematics and Physics,* Vol. 32, July–Oct. 1953, pp. 83–101.

[7]Dean, W. R., "On the Steady Motion of Viscous Liquid Past a Flat Plate,"*Mathematika,* Vol. 1, No. 2, Dec. 1954, pp. 143–156.

[8]Sato, H. and Kuriki, K., "The Mechanism of Transition in the Wake of a Thin Flat Plate Placed Parallel to a Uniform Flow," *Journal of Fluid Mechanics,* Vol. 11, Nov. 1961, pp. 321–352.

[9]Dennis, S. C. R. and Dunwoody, J., "The Steady Flow of a Viscous Fluid Past a Flat Plate," *Journal of Fluid Mechanics,* Vol. 24, March 1966, pp. 577–595.

[10]Davis, R. T., "Laminar Incompressible Flow Past a Semi-Infinite Flat Plate," *Journal of Fluid Mechanics,* Vol. 27, March 1967, pp. 691–704.

[11]Plotkin, A. and Flugge-Lotz, I., "A Numerical Solution for the Laminar Wake Behind a Finite Flat Plate," *Transactions of ASME, Journal of Applied Mechanics,* Vol. 35, Dec. 1968, pp. 625–630.

[12]Stewartson, K., "On the Flow Near the Trailing Edge of a Flat Plate," *Proceedings of the Royal Society of London,* Vol. A306, 1968, pp. 275–290.

[13]Stewartson, K., "On the Flow Near the Trailing Edge of a Flat Plate II," *Mathematika,* Vol. 16, No. 31, June 1969, pp. 106–121.

[14]Messiter, A. F., "Boundary-Layer Flow Near the Trailing Edge of a Flat Plate," *SIAM Journal of Applied Mathematics,* Vol. 18, No. 1, 1970, pp. 241–257.

[15]Talke, F. E. and Berger, S. A., "The Flat Plate Trailing Edge Problem," *Journal of Fluid Mechanics,* Vol. 40, Jan. 1970, pp. 161–189.

[16]Callens, E. E., "A Time-Dependent Approach to Fluid Mechanical Phenomelogy," AIAA Paper 70-46, 1970.

[17]Van de Vooren, A. I. and Dijkstra, D., "The Navier-Stokes Solution for Laminar Flow Past a Semi-Infinite Flat Plate," *Journal of Engineering Mathematics,* Vol. 4, No. 1, 1970, pp. 9–27.

[18]Schneider, L. I. and Denny, V. E., "Evolution of the Laminar Wake Behind a Flat Plate and Its Upstream Influence," *AIAA Journal,* Vol. 9, April 1971, pp. 655–660.

[19]Jobe, C. E. and Burggraf, O. R., "The Numerical Solution of the Asymptotic Equations of Trailing Edge Flow," *Proceedings of the Royal Society of London,* Vol. A340, 1974, pp. 91–111.

[20]Veldman, A. E. P. and Van de Vooren, A. I., "Drag of a Finite Flat Plate," *Lecture Notes in Physics,* Vol. 35, 1975, pp. 422–430.

[21]Melnik, R. E. and Chow, R., "Asymptotic Theory of Two-Dimensional Trailing-Edge Flows," NASA SP-347, 1975, pp. 177–250.

[22]Thompson, J. F., Thames, F. C., Walker, R. L., and Shanks, S. P., "Numerical Solutions of the Unsteady Navier-Stokes Equations for Arbitrary Bodies Using Boundary-Fitted Curvilinear Coordinates," *Unsteady Aerodynamics, Proceedings of Symposium Held at Univ. of Arizona,* edited by R. B. Kinney, March 1975, pp. 453–485.

[23]Nishioka, M. and Miyagi, T., "Measurements of Velocity Distributions in the Laminar Wake of a Flat Plate," *Journal of Fluid Mechanics,* Vol. 84, Feb. 1978, pp. 705–715.

[24]Dwoyer, D. L., "Application of a Velocity-Split Navier-Stokes Solution Technique to External Flow Problems," AIAA Paper 79-1449, 1979.

[25]Miyagi, T. and Nishioka, M., "Oseen Velocity Distributions in the Wake of a Flat Plate," *Journal of Fluid Mechanics,* Vol. 97, March 1980, pp. 145-155.

[26]Veldman, A. E. P., "Boundary Layers with Strong Interaction: From Asymptotic Theory to Calculation Method," *Proceedings of BAIL 1 Conference,* Trinity College, Dublin, 1980, p. 149.

[27]Walter, K. T. and Larsen, P. S., "The FON Method for the Steady Two-Dimensional Navier-Stokes Equations," *Computers and Fluids,* Vol. 9, No. 3, Sept. 1981, pp. 365-376.

[28]Rubin, S. G. and Reddy, D. R., "Global PNS Solutions for Laminar and Turbulent Flow," AIAA Paper 83-1911, 1983.

[29]Werle, M. J. and Verdon, J. M., "Solutions for Laminar Subsonic Trailing Edge Flows at Asymptotically Large Reynolds Numbers," *Proceedings of BAIL 1 Conference,* Trinity College, Dublin, June 1980, pp. 164-178.

[30]Varley, E., "An Approximate Boundary Layer Theory for Semi-Infinite Cylinders of Arbitrary Cross-Section," *Journal of Fluid Mechanics,* Vol. 3, March 1958, pp. 601-614.

[31]Stewartson, K. and Howarth, L., "On the Flow Past a Quarter Infinite Plate Using Oseen's Equations," *Journal of Fluid Mechanics,* Vol. 7, Jan. 1961, pp. 1-21.

[32]Elder, J. W., "The Flow Past a Flat Plate of Finite Width," *Journal of Fluid Mechanics,* Vol. 9, Sept. 1960, pp. 133-153.

[33]Chen, H. C. and Patel, V. C., "Laminar Flow at the Trailing Edge of a Flat Plate," *AIAA Journal,* Vol. 25, July 1987, pp. 920-928.

[34]Xu, Y. N. and Chen, C. J., "Finite Analytic Numerical Prediction of Laminar and Turbulent Flows Past a Thin Finite Flat Plate," *Midwestern Mechanics Conference,* Purdue Univ., West Lafayette, IN, 1987, pp. 519-524.

[35]Reddy, J. N., "On Penalty Function Methods in the Finite Element Analysis of Flow Problems," *International Journal on Numerical Methods for Fluids,* Vol. 2, No. 2, 1982, pp. 151-171.

[36]Engelman, M. S., "FIDAP: A Fluid Dynamics Analysis Program," *Advances in Engineering Software,* Vol. 4, 1982, p. 163.